Tellus (1987), *39A*, 408–425

A subsynoptic vortex over the Mediterranean with some resemblance to polar lows

By ERIK RASMUSSEN, *Geophysical Institute, Meteorological Department, University of Copenhagen, Haraldsgade 6, DK-2200 Copenhagen N, Denmark* and CHRISTIAN ZICK, *Free University Berlin, Audiovisual Center, Malteserstr. 74-100, D-1000 Berlin 46, Germany*

(Manuscript received 7 July 1986; in final form 14 January 1987)

ABSTRACT

The development of a subsynoptic vortex over the Mediterranean has been followed for several days (27 September–1 October 1983). The major tool for the study are METEOSAT images from the visible and infrared spectrum, and wind data from low and high levels obtained by tracking cloud elements in these images. The subsynoptic vortex forms in the central part of a synoptic scale low of modest intensity, and deep convection is observed in the region prior to the formation of the vortex. The initial formation of the vortex is most probably caused by a rapid spin-up due to intense convection of pre-existing vorticity associated with the synoptic scale low. After its formation, the vortex moves in a large circle and is best developed at a position over the sea west of Sardinia and Corsica. The vortex at this time is characterized by deep convection, a vertical axis and an upper-level anticyclonic divergent flow corresponding to a warm core structure.

1. Introduction

Hurricane-like cyclones are known sometimes to form over the Mediterranean (Ernst and Matson, 1983; Billing et al., 1983). In the present work we will consider a development of a vortex from September 1983 which in many ways resembles polar lows of the type which often develops over the Norwegian Sea near Bear Island (Rasmussen, 1985). The same case has been considered by Mayengon (1984).

One of the mechanisms responsible for the development of polar lows is convection. On the other hand more-or-less shallow baroclinic zones are almost invariably present in the regions where polar lows form, and it is difficult to assess the relative importance of convection versus baroclinic instability. In the present case, however, baroclinic instability does not seem to play any role at all, and for this reason, we in some respects may consider this as an "ideal" development of a polar low of the convective type.

2. Cloud track wind data

Since half-hourly image sequences from meteorological geostationary satellites became available, it has been repeatedly verified (METEOSAT Operations Advisory Group, 1979; Shenk and Kreins, 1970; Hasler et al., 1976), that cloud displacements in many cases may be used to evaluate the wind at cloud level. Such cloud winds have been proved to be useful for synoptic scale analysis in data-sparse regions like over the oceans, and for subsynoptic scale analysis (Zick, 1983). A remaining problem, however, is to assign the observed cloud motion winds to a specific pressure level. Generally the satellite-observed radiation temperature of the cloud top is compared with any available vertical temperature-pressure distribution, and the cloud wind is then assigned to the relevant pressure level. In our investigation, the "Interactive System Meteorology" ISM of DFVLR/Oberpfaffenhofen (Deutsche Forschungs- und Versuchsanstalt für Luft- und Raumfahrt, German Aerospace

Research Establishment) has been used. This system defines the pressure level of the cloud by comparing the cloud top radiation temperature with climatological temperature profiles. Due to differences between the climatological distribution and the actual one, the cloud level winds may sometimes be assigned to a wrong pressure level. Furtheron, the radiation temperature may be contaminated by radiation originating from layers below when the target is partly transparent (semi-transparent cirrus clouds) resulting in a too low pressure level assignment. Finally, even if the computed pressure levels of the cloud tracers were correct, they still would be distributed in a more or less deep layer. Thus for practical reasons we simply apply the cloud winds at the standard isobaric surfaces which are most close to the levels where we find the majority of cloud winds.

As will be demonstrated, such cloud wind data are very useful and an indispensable data supplement for the analysis of subsynoptic weather systems.

2.1. The upper air wind data used in the case study

METEOSAT VIS- and IR-images, each day from 11.30, 12.00, and 12.30 GMT, were used for deriving the wind data. High level wind data were derived from the IR-triplet, using operator-controlled cross correlation techniques similar to the techniques used in the McIDAS system (Suomi, 1975). Low level cloud displacements were tracked from the VIS image data using a single-point tracking metric, since the rapid change of the low level cloud structures may cause poor cross correlation results. The tracers were selected by the operator who decided subjectively whether an observed cloud motion wind should be assigned to either the low level or the high level motions.

Table 1 shows the distribution of the objective height assignment of the wind data as performed by the ISM: the high level wind data, as expected, have a clear maximum at 300 mb, but also a secondary maximum around 950 mb. This is typical for high level cloud wind data computed from semi-transparent cirrus clouds. 66% of the assigned low level wind data are found between 750 and 900 mb, but a relatively high number of low level tracers are assigned to higher levels. Hasler et al. (1976) showed, however, that wind data derived from tracking convective clouds fit best to the level of the cloud base, i.e., a lower height than that derived from the radiation temperature of the cloud top. All high level cloud wind data are therefore analysed together with the 300 mb radiosonde winds, and the low level cloud wind data together with the 850 mb radiosonde winds. These analyses will be referred to as "high level" and "low level" in order to distinguish them from 300 mb or 850 mb upper air analyses. 546 upper air wind data were used for the analysis of the period 27 September through 1 October 1983. 145 of these winds were radiosonde winds, and 398 satellite winds. The low level wind data set of 12.00 GMT 30 September 1983, was the only one which was augmented by three gradient winds computed from the pressure gradient at sea level. This was necessary, because analyses of the original data set showed a rotation center at a wrong position, due to no cloud tracers being available close to the western side of the rotation center.

Each set of wind data was interpolated to grid points with half-degree intervals. From these grid point values, streamlines, fields of relative vorticity and divergence were computed.

Table 1. *ISM-performed objective tracer-height assignment of the satellite wind data*

Pressure (mb)	Low-level winds	High-level winds
100	–	2
150	–	6
200	–	7
250	–	23
300	–	53
350	–	31
400	3	29
450	2	14
500	3	18
550	6	9
600	8	1
650	8	1
700	12	1
750	21	–
800	30	1
850	22	–
900	26	3
950	6	10
1000	2	3
unassigned:	11	26

3. The development of the subsynoptic scale vortex

The phenomenon to be discussed in this paper is a subsynoptic vortex-like disturbance which initially was formed in the western region of a low of modest intensity between Sicily and northern Tunisia. Note that in the following we will generally use the term "vortex" for the subsynoptic system.

The upper air synoptic situation in the region during our period of interest is dominated by the formation of a deep, cold cut-off low. The low initially formed when a short-wave trough was cut off from the westerly current further north. The 300 mb map showing the position of the cut-off low at 00.00 GMT 28 September is shown in Fig. 1, together with the 1000/500 mb thickness field. The position of the vortex at the surface is indicated by "V", which is in the very center of the cold dome.

3.1. 27 September

The initial formation of the vortex at the surface is indicated by strong pressure falls, a west-south-westerly wind and heavy rainfall at Carthage (see Fig. 10 for the position of this and other places mentioned in the text) at 15.00 GMT 27 September (Fig. 2a). Prior to that time there is no indication of the vortex at the surface maps. However, a small region of intense convection indicated by very low cloud top temperatures can be seen at 12.00 GMT 27 September (Fig. 3) over the region where signs of the vortex formation can be observed in the surface map three hours later (Fig. 2a). The analyses of the high level and low level wind fields (not shown) indicate upper level divergence and a low-level secondary center of positive relative vorticity in the region where the vortex formation subsequently takes place. At 15.00 GMT the METEOSAT image (not shown) exhibits almost the same large scale cloud spiral as three hours before (Fig. 3) but in addition it also shows a small notch in the cloud field just north of Carthage. Already 3 hours later, at 18.00 GMT, the vortex is clearly seen on the METEOSAT image (Fig. 4). Though strong pressure falls are observed at Carthage at 15.00 GMT, the wind speed at that time is still only 7 m s^{-1}. However, already at 16.15 GMT, the wind speed has increased to 22 m s^{-1} (from the west) which is the highest wind speed observed at Carthage on 27 September, according to information from l'Institut National de la Météorologie Tunisienne.

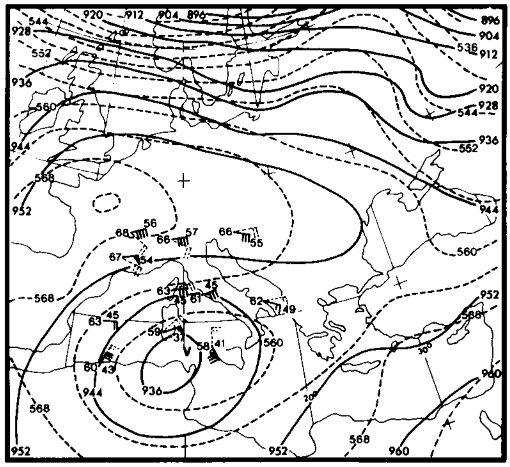

Fig. 1. 300 mb (solid lines) and 1000/500 mb thickness (dashed lines), 00.00 GMT 28 September 1983, showing a cold cut-off low over the western Mediterranean. Contour and thickness lines in decameters. 300 mb heights are written to the right of the stations and the thickness to the left, both in decameters and first cipher omitted. Winds are given in the conventional way. The position of the subsynoptic vortex is indicated by "V". Reproduced from "Europäischer Wetterbericht" of the "Deutscher Wetterdienst".

3.2. 28 September

As the vortex moves towards Sardinia (see Fig. 10) surface winds around 15 and 20 m s^{-1} are reported close to the low pressure center (see Figs. 2b, c). The ship near the low pressure center at 06.00 GMT 28 September reports wave heights of four meters (Mayengon, 1984) and the pressure in the center of the low is close to 1000 mb. This low value of the center pressure (see Fig. 11) will be further discussed in Section 4.

The NOAA image (Fig. 5) illustrates that the large scale frontal cloud band is dissolving and shows, in the very center of the cloud spiral, a cloud-free spot, similar to an "eye".

Both the surface observations (Fig. 2b) and the NOAA image show the contraction of the cyclonic activity into the central part of the low, and so do the low level and high level analyses of the relative vorticity at 12.00 GMT (Figs. 6a, b). Compared to the situation 24 hours before (not

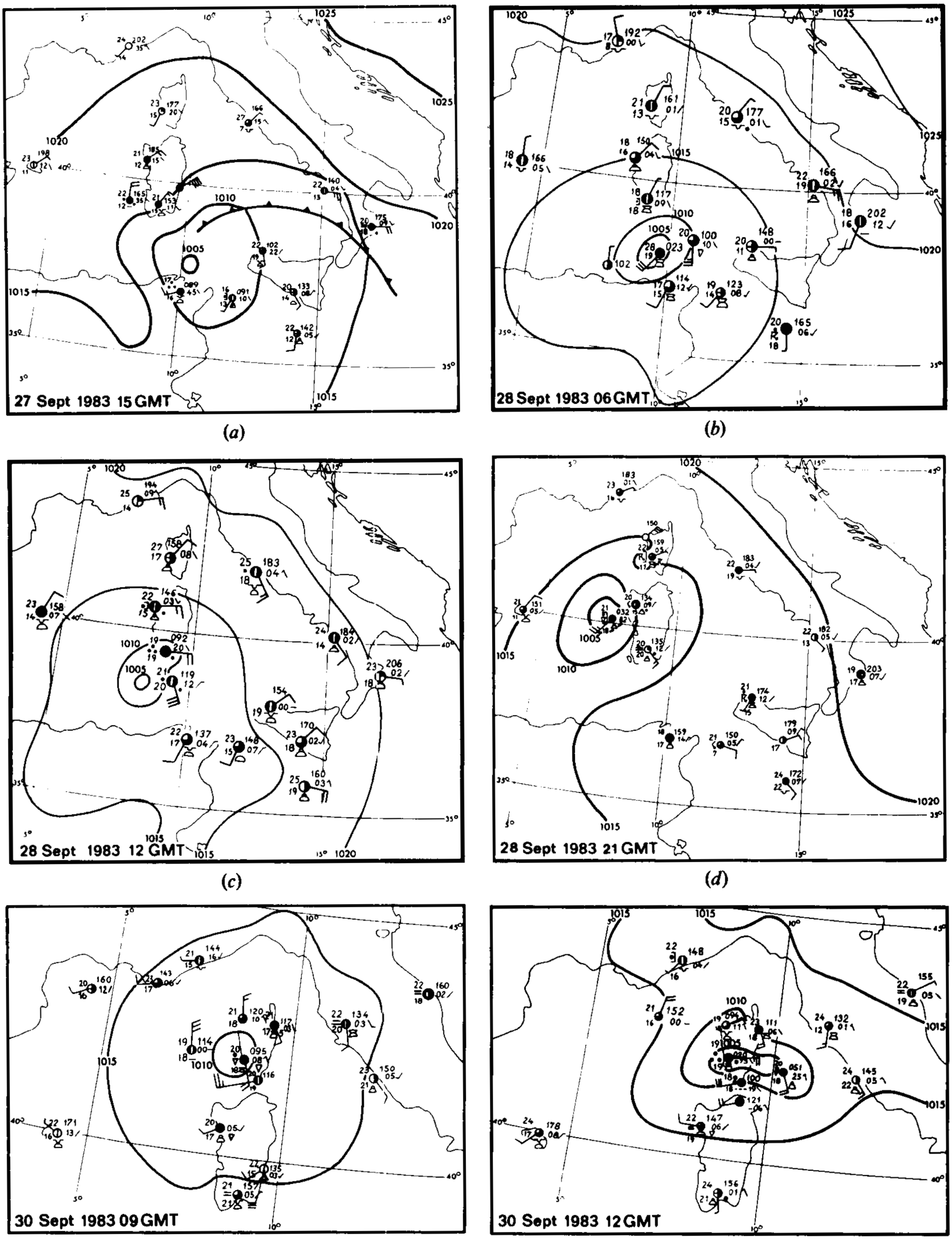

Fig. 2. Surface maps 15.00 GMT 27 September through 12.00 GMT 30 September 1983, showing the subsynoptic vortex in the western Mediterranean. The surface analyses are based on all available observations in the region. Only a few observations have been plotted on the maps shown.

shown), the maximum low level vorticity has increased from 15 to $30 \cdot 10^{-5}$ s^{-1} and is now situated quite close to the surface low (Fig. 2c). The high-level vorticity over the center of the low is only half the intensity observed 24 hours before. The decrease of the high level cyclonic rotation over the central part of the surface low probably is a consequence of a warming of the core region of the low, a hypothesis which will be elaborated in Section 4.

3.3. 29 September

During 29 September, the vortex is over the sea west of Sardinia and Corsica (see Fig. 10). There are no ship observations in the immediate surroundings of the vortex at this time and the center positions are partly based on continuity with preceeding and following maps as well as on satellite images. The NOAA image of 14.18 GMT 29 September (Fig. 7) shows a tight and almost circular mesoscale cloud vortex while the frontal cloud bands have almost disappeared.

The low-level vorticity maximum (Fig. 6c) is still around $30 \cdot 10^{-5}$ s^{-1}, but the isopleths are now much more symmetric and centered around the surface low. It must be noted that the low level cloud winds are only available in the outer region of the vortex so that the analysis on the subsynoptic scale at this time is a little uncertain. The position of the vorticity maximum, however, coincides with the surface position of the low which was found independently from the low level wind analysis. The high level vorticity (Fig. 6d) has become *negative* with a minimum above the position of the surface low. The negative vorticity reflects the anticyclonic curvature of the high level stream lines (Fig. 8b). Note that apart from the area close to the vortex the upper level

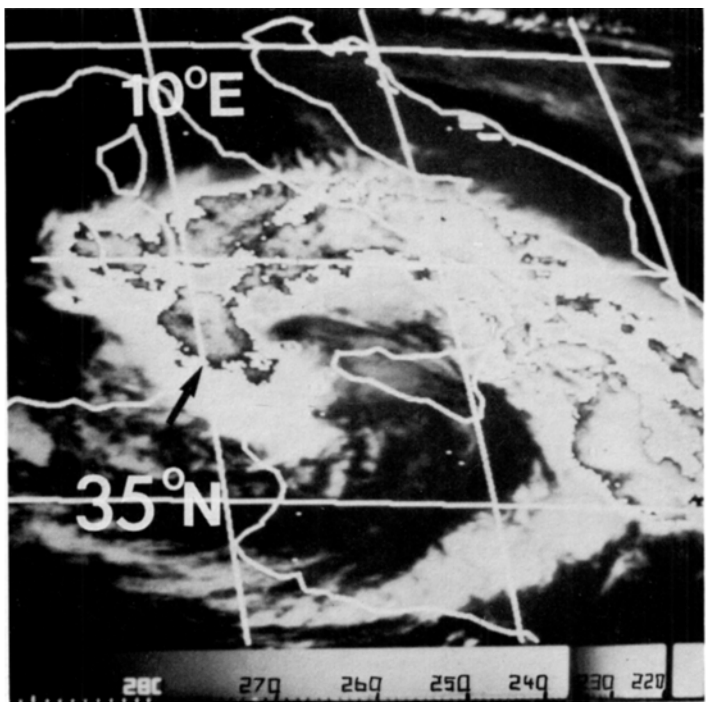

Fig. 3. METEOSAT infrared satellite image, 12.00 GMT 27 September 1983, showing the large scale cloud spiral associated with the synoptic scale low in which the subsynoptic vortex forms. The arrow shows the region of deep convection where the subsynoptic vortex is observed 3 hours later. A white-to-black-breakpoint at $-38\,^{\circ}C$ in the enhancement of the grey scale has been applied in order to display the high level clouds in more detail. Highest cloud tops (white) have equivalent black-body temperatures of -52 to $-54\,^{\circ}C$. Received by: ESA-ESOC, Darmstadt, processed on ISM-3, ZEAM.

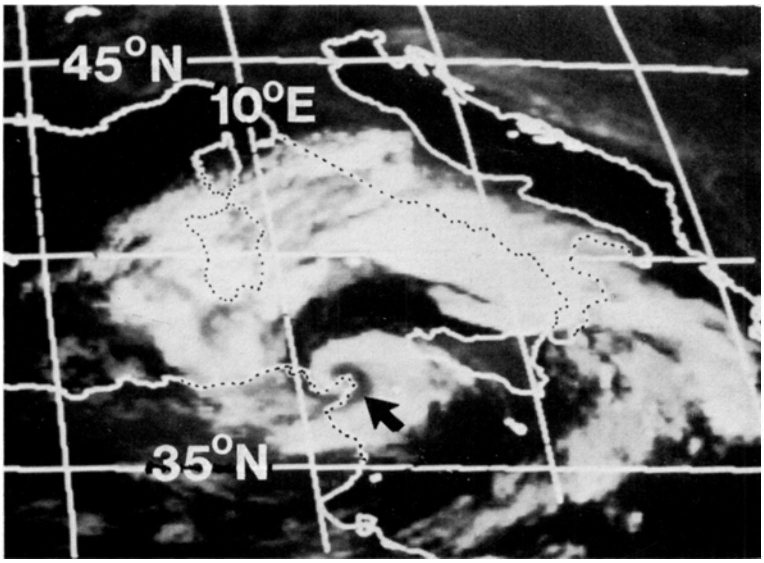

Fig. 4. METEOSAT infrared satellite image, 18.00 GMT 27 September 1983, showing the subsynoptic vortex (at the arrow) over the sea close to Carthage. Received by: ESA-ESOC, Darmstadt, processed on ISM-3, ZEAM.

flow continues to be cyclonic. Corresponding to the region with upper level anticyclonic flow and negative relative vorticity we find an area with high level divergence (Fig. 8a) centered in the cirrus outflow region. On the two preceding days, the upper level divergence fields (not shown) were either irregularly weakly divergent or convergent in the core area.

The cirrus shield associated with the vortex in Fig. 7 indicates deep and strong convection. On a NOAA image from 19.10 GMT (not shown) this cirrus shield has partly disappeared indicating less convective activity than in the preceeding hours.

3.4. 30 September

As the surface low moves east towards Corsica, several ship observations become available close to the center. At 09.00 GMT (Fig. 2e), a 15 m s^{-1} wind from north is reported 150 km west of Ajaccio, while Ajaccio itself reports south, 10 m s^{-1}. Three hours later, at 12.00 GMT (Fig. 2f), the low pressure center has made landfall accompanied by a strong pressure drop (see Fig. 11). At the same time, a second low pressure center already has formed east of Corsica. Note by comparing Figs. 2e, f that the strong pressure drop at Ajaccio at 12.00 GMT (7.5 mb in 3 hours) is not due to advection alone, but mostly to a deepening of the center. When the original low pressure center crosses the 2200 m mountains of southern Corsica, it starts to fill but strong winds of 20 m s^{-1} still blow from the west in the Strait of Bonifacio between Corsica and Sardinia.

The landfall shortly before noon also has a strong influence on the upper air flow. At low levels, the vorticity at 12.00 GMT (Fig. 6e) reaches its maximum with values close to $45 \cdot 10^{-5}$ s^{-1}. It is even more remarkable that the upper region of anticyclonic (negative) relative vorticity observed on 29 September (Fig. 6d) now has changed to strong cyclonic (positive) relative vorticity (Fig. 6f). Corresponding to this change we observe strong upper level convergence in the same region (Fig. 8c). The corresponding METEOSAT-IR image (not shown) shows that deep convective clouds are still present. However, cloud top temperatures are slightly warmer (~ -48 °C) than on 29 September (~ -54 °C, see Fig. 14). The high level stream lines (Fig. 8d) show pronounced cyclonic curvature over the center of the low. This change in the structure of the system is further discussed in Section 4.

3.5. 1 October

The surface pressure at the center of the vortex

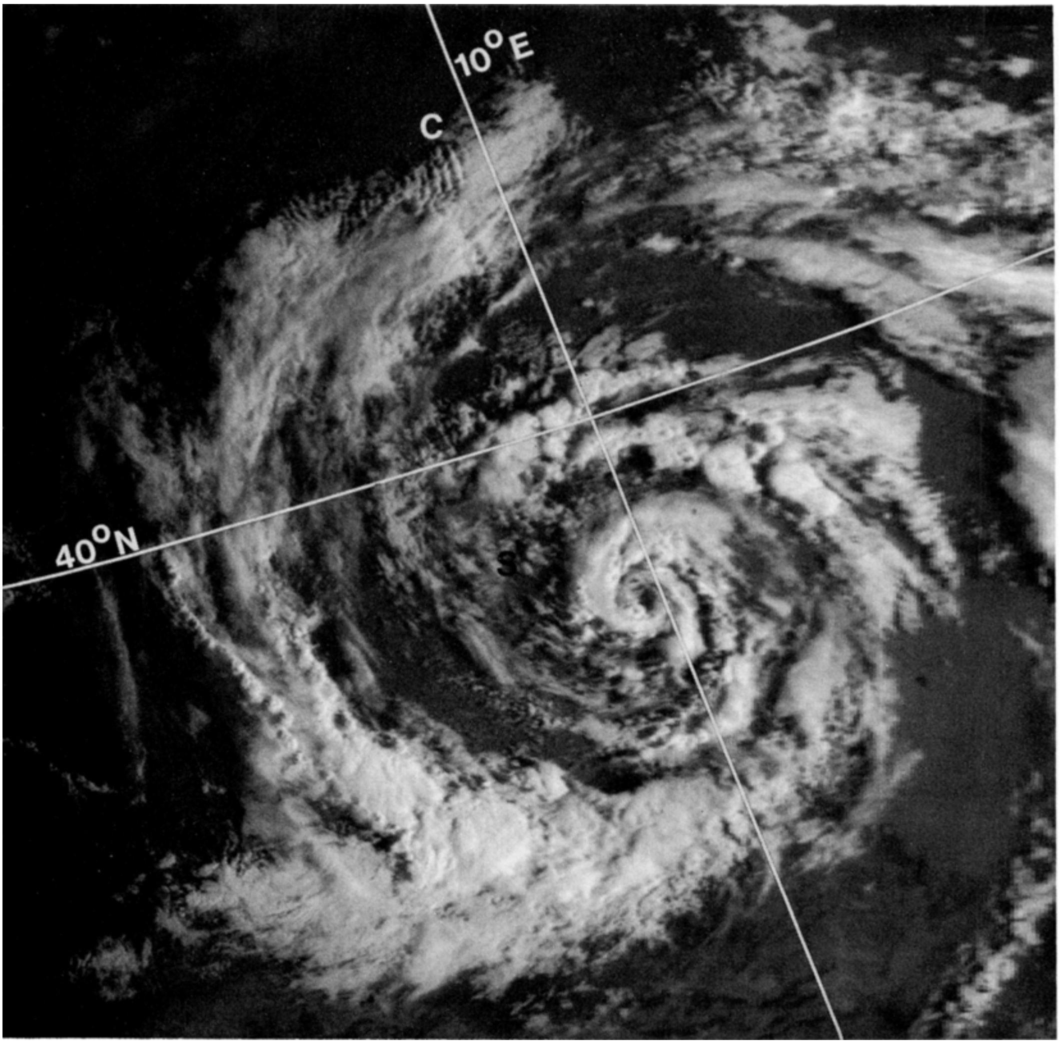

Fig. 5. NOAA-7, visible channel satellite image, 08.07 GMT 28 September 1983, showing the dissolving large scale cloud spiral with the subsynoptic vortex in its center. The southern tip of Sardinia has been marked by "S" and the northern tip of Corsica by "C". Photograph courtesy of Department of Electrical Engineering and Electronics, University of Dundee.

slowly increases to 1011 mb at 12.00 GMT 1 October, when the vortex travels southwards between Sardinia and Italy, but surface winds of 15 m s^{-1} are still reported in the vicinity of the low pressure center. Accordingly, the low level vorticity analysis (not shown) still shows values of $30 \cdot 10^{-5}$ s^{-1} in the center. The intensity of the high level vorticity (not shown) has decreased to about $12 \cdot 10^{-5}$ s^{-1}, and the high-level divergence pattern (not shown) is disintegrating. A NOAA image from 13.54 GMT 1 October (Fig. 9) shows that the clouds associated with the vortex at this time are much more shallow than on the preceeding days except for one cumulonimbus complex close to the center. In the following hours, the vortex further weakens until it finally decays after landfall near Tunis, North Africa, in the morning of 2 October.

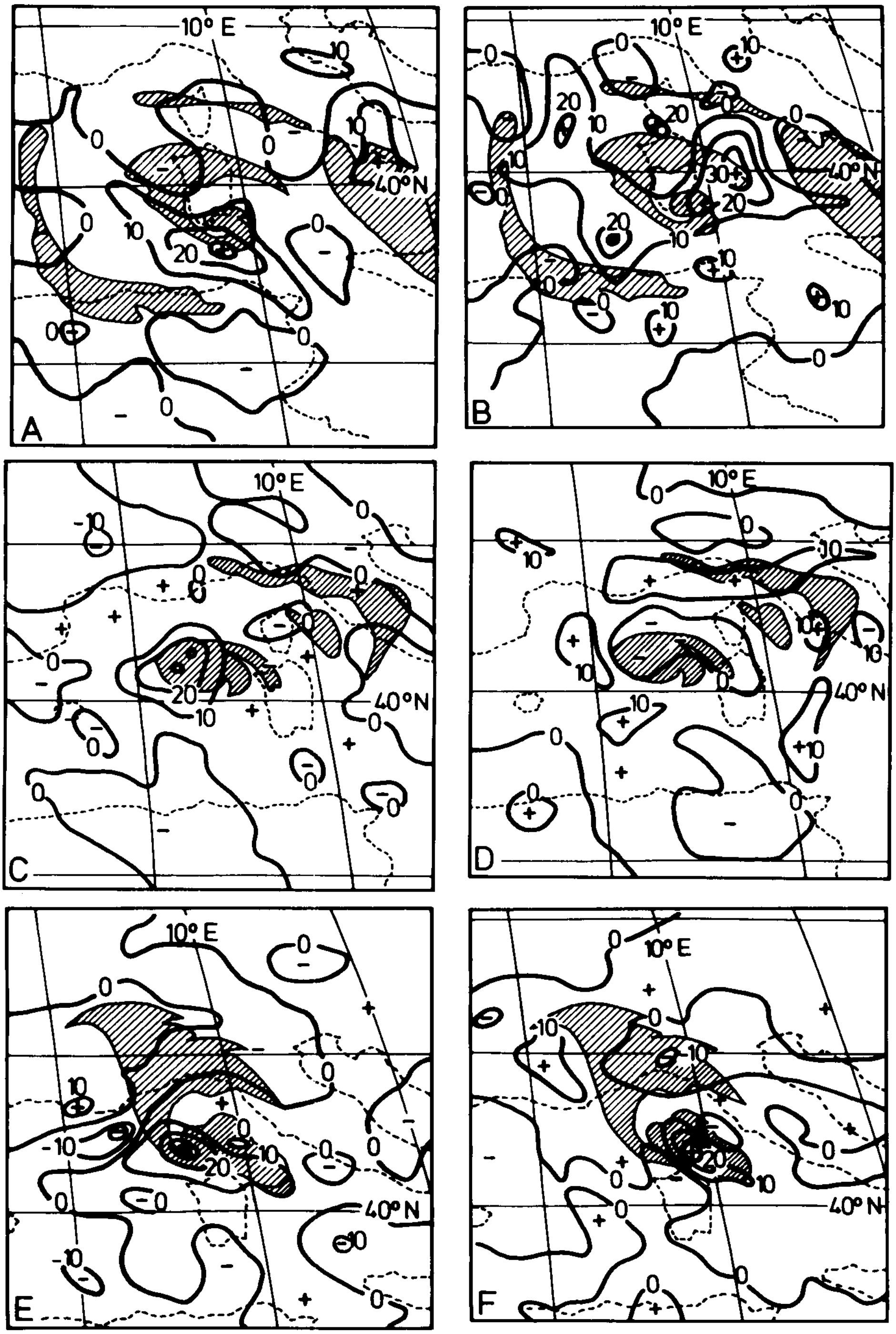

Fig. 6. ISM-performed analyses of the relative vorticity in units of 10^{-5} s^{-1}. High level clouds are shown schematically by the hatched areas. The left side shows the low level (~850 mb) analyses and the right side the high level (~300 mb) analyses. (a) and (b): 12.00 GMT 28 September 1983. (c) and (d): 12.00 GMT 29 September 1983. (e) and (f): 12.00 GMT 30 September 1983.

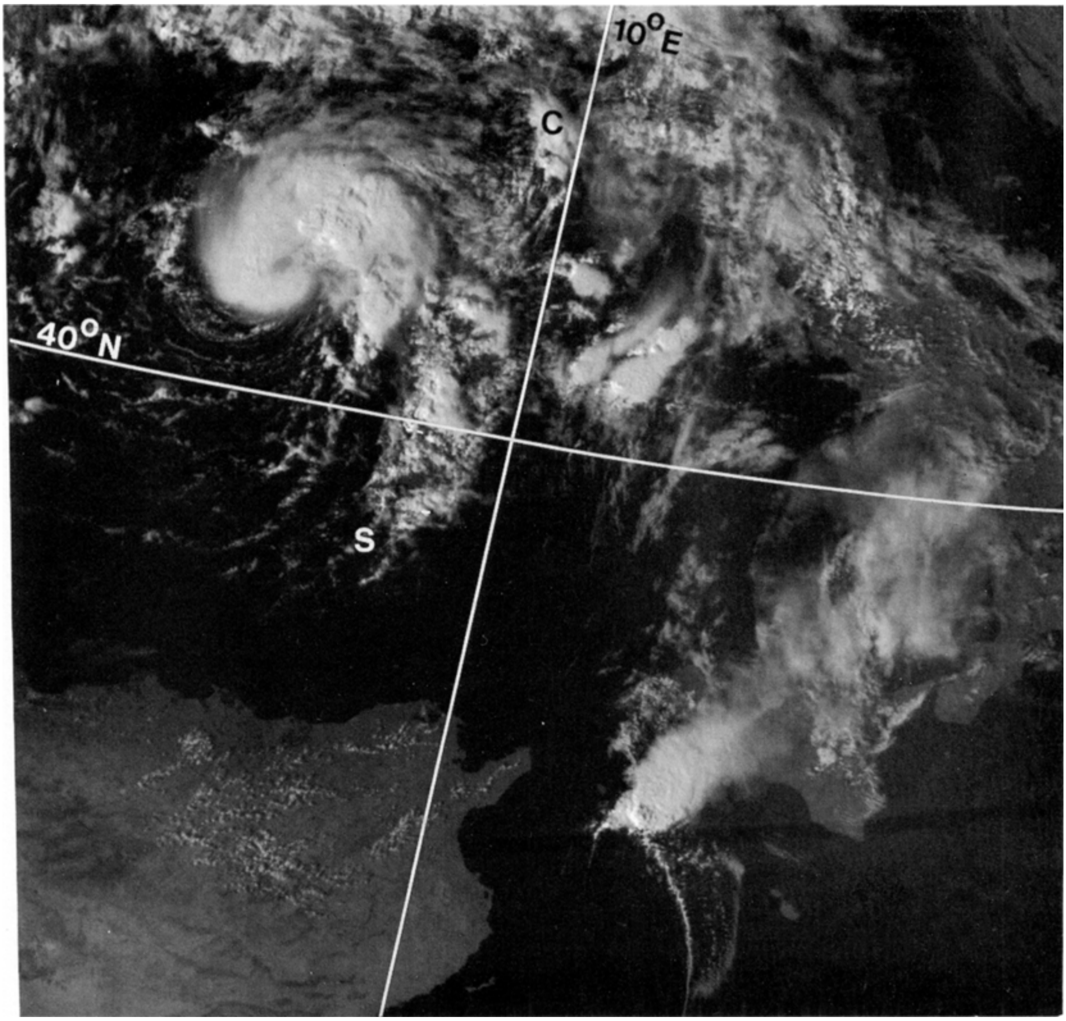

Fig. 7. NOAA-7, visible channel satellite image 14.18 GMT 29 September 1983, showing the vortex at the time when it is best developed. The southern tip of Sardinia is shown by "S", and the northern tip of Corsica by "C". Photograph courtesy of Department of Electrical Engineering and Electronics, University of Dundee.

4. Dynamics of the vortex

In this section, we have tried to interpret the existing observations including the rather detailed wind fields.

4.1. The dynamics of the vortex as reflected in the surface data

After the formation of the vortex near the northern coast of Tunisia, it completes a large circle in about 4 days and finally dissolves after having made landfall close to its place of origin (Fig. 10). An inspection reveals oscillations especially in the surface pressure, which will be discussed in the following.

As usual, it is possible to describe the surface pressure field with more confidence than the wind field and accordingly we will use two parameters derived from pressure observations to describe the intensity of the vortex.

The first parameter, the center pressure, is shown as a function of time (Fig. 11a). It is not drawn as a continuous curve, because a close inspection of the satellite images and the surface

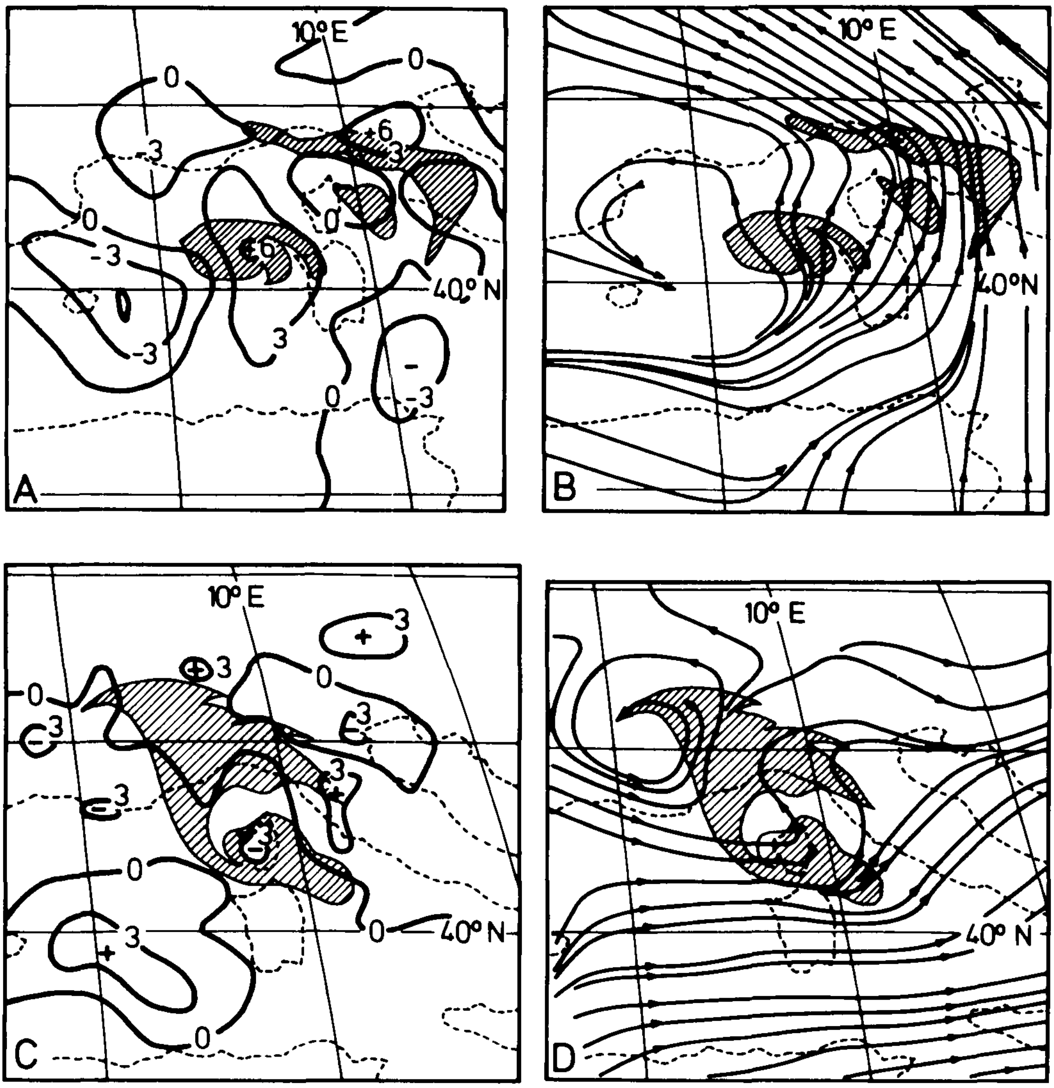

Fig. 8. ISM-performed high level (~300 mb) analyses of the divergence (10^{-5} s^{-1}, left) and stream lines (right). High-level cloud contours are shown schematically by the hatched areas. Figs. (a) and (b): 12.00 GMT 29 September 1983. Figs. (c) and (d): 12.00 GMT 30 September 1983.

maps show that the center two times makes landfall (not including the final one at Tunisia on 2 October), and on both occasions the centers rapidly dissolve. New centers, however, form almost simultaneously close to the old ones but over the sea (see Fig. 10).

The second parameter used is the mean diameter of the (closed) 1010 mb isobar (Fig. 11b) up to 06.00 GMT 1 October. Beyond that, the pressure in the center is above 1010 mb.

Some interpolation has been necessary to construct Fig. 11. However, we consider the curves as fairly realistic, although some details in Fig. 11a may be lost due to lack of data, especially between 00.00 and 15.00 GMT 29 September.

Between 03.00 and 06.00 GMT 28 September, the center pressure drops about 5 mb. Similar and even stronger pressure falls are, as seen from Fig. 11, observed after the two landfalls. The METEOSAT image from 06.00 GMT 28 Septem-

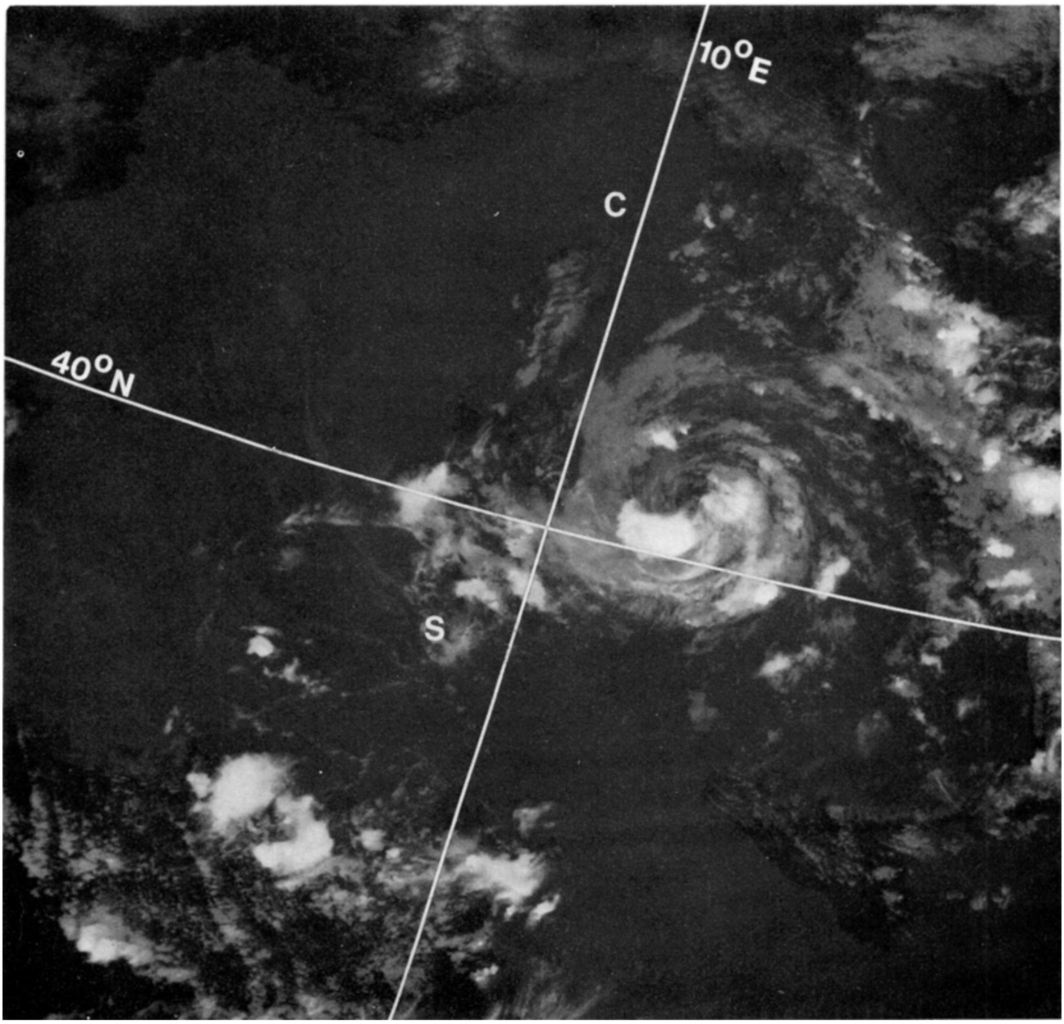

Fig. 9. NOAA-7 infrared satellite image 13.54 GMT 1 October 1983, showing the vortex after the crossing of Corsica. The southern tip of Sardinia is shown by "S" and the northern tip of Corsica by "C". Photograph courtesy of Department of Electrical Engineering and Electronics, University of Dundee.

ber (not shown) exhibits a tight mesoscale cloud vortex in the center of the subsynoptic vortex. Judging from other (not shown) METEOSAT images the mesoscale vortex at 06.00 GMT is somewhat better organized and associated with deeper convection than it is three hours before as well as 3 hours later.

Elementary calculations which will be elaborated later on in Subsection 4.2 show that even small changes in the mean temperature between the surface and the tropopause will cause relatively large changes in the surface pressure provided the atmosphere is hydrostatic. Such changes in the mean temperature can easily be explained as the result of changes in the intensity of the convection in the central region of the vortex and may thus explain the observed pressure falls.

During the period after the first landfall, the vortex is situated over the warm sea, far away from any coastlines. The vortex is symmetric, tight, and has a warm core due to intense

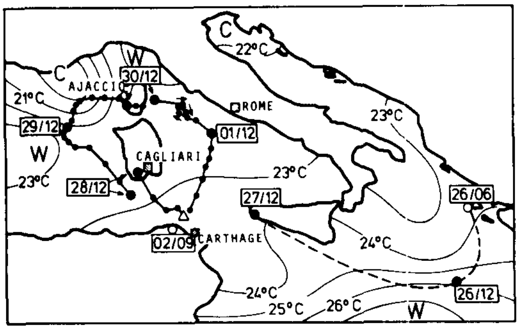

Fig. 10. Track of the initial low pressure center (dashed line) and the vortex low pressure center (solid line) at the surface (with date/GMT annotations). 3-hourly positions are marked by small dots, the triangle north of Carthage marks the position of the vortex from 15.00 GMT 27 September through 00.00 GMT 28 September 1983. Sea surface temperature analysis of 28 September 1983, is based on METEOSAT measurements and ship observations. Positions of stations mentioned in the text are indicated.

convection. The warm core at this time manifests itself through the anticyclonic divergent upper level flow (Fig. 8a, b) as well as through the low surface pressure, $\sim$1000 mb, in the central part of the low. The pressure deficit between the inner core and the environment is of the order of 10 mb, and is closely related to the temperature of the warm core. This point will be also elaborated in Subsection 4.2. Later on, at 00.00 GMT 1 October, the warm core can be directly observed in the thickness field (Fig. 12).

After 15.00 GMT 29 September, the center pressure starts to rise (Fig. 11a). This happens when the vortex has reached a region with relatively low sea surface temperatures (see Fig. 10), and when the cirrus shield has started to diminish. The difference of the sea surface temperatures between the vortex position at 06.00 GMT 29 September and the position at 00.00 GMT 30 September is about 2.5°C. If the temperature of ascending surface air is changed by a similar amount, then the warm core will be strongly affected (see Subsection 4.2).

As an immediate consequence of the second landfall (30 September, around 12.00 GMT) the center pressure deepens significantly but transiently from 1008 mb to about 1001 mb within only three hours. This rather paradoxial result must be considered as the consequence of an enhanced low level inflow in the boundary layer towards the center of the vortex due to the highly increased friction over the mountainous island. The increased inflow and the associated forced lifting will induce additional convective activity which explains the observed pressure fall. As the center proceeds inland the pressure again begins to rise.

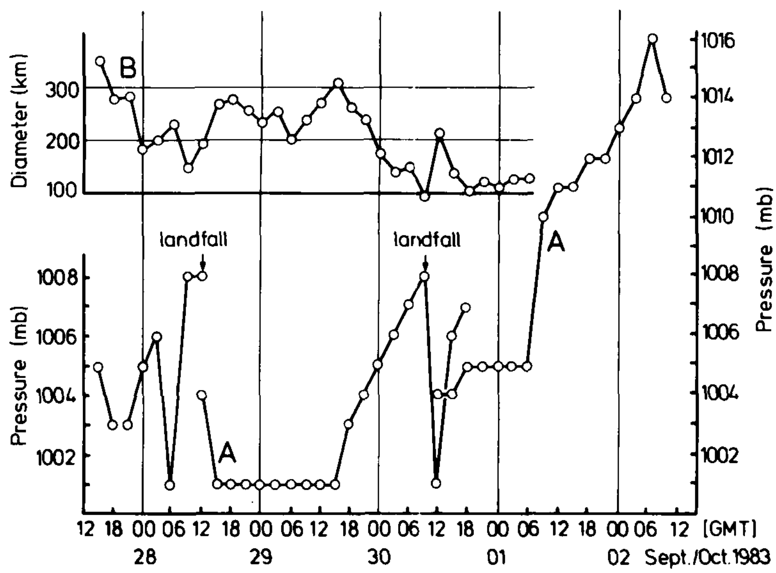

Fig. 11. The center pressure of the vortex (A) and the variation of the mean diameter of the closed 1010 mb isobar around the vortex center (B) as functions of time.

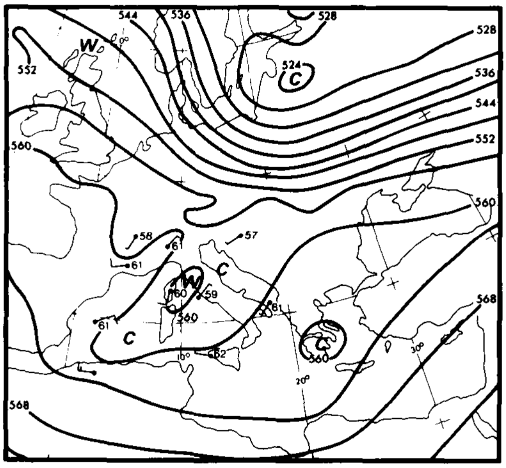

Fig. 12. 500/1000 mb thickness analysis, 00.00 GMT 1 October 1983, showing the warm core of the vortex between Corsica and Italy. Reproduced with minor changes from the "Europäischer Wetterbericht" of Deutscher Wetterdienst (DWD).

Three times during the life-time of the vortex, the surface pressure in its center drops to around 1000 mb. This happens temporarily on 06.00 GMT 28 September, then from 15.00 GMT 28 September to 15.00 29 September, and again temporarily on 12.00 GMT 30 September (see Fig. 11a). These pressure drops occur at widely different places and probably all reflect the maximum possible pressure fall due to convective warming in the center region (see Subsection 4.2).

After the re-establishment of the vortex after the second landfall, the center pressure rises steadily. This is consistent with the fact that the convection has now become less intense.

4.2. *Thermodynamic features*

The ambient atmosphere in which the vortex develops and exists for more than four days is rather homogeneous. This can be illustrated by for example the 500/1000 mb thickness field from 00.00 GMT 1 October (Fig. 12). The warm core associated with the vortex is marked by "W" and is situated in the central part of a homogeneous and relatively cold air mass. Obviously, this and other thickness analyses are on a (large) synoptic scale and generally cannot resolve the sub-synoptic vortex. On 1 October, however, the vortex is situated in a position close to two radiosonde stations, and at this time the warm core in the thickness field can be recognized between Corsica and the Italian coast.

During its track around Sardinia and Corsica the vortex is never far away from the radiosonde stations in the region. The Cagliari radiosonde ascent of 12.00 GMT 28 September took place close to the center of the vortex and seven other ascents took place at distances from the center varying from 120 km to 260 km. The temperature distributions of the seven radiosonde ascents in the outer part of the vortex are remarkably similar even if the distance from the center to the place of the ascent varies considerably. Because of the small scatter of the temperature values it is meaningful to construct a mean or composite sounding from the seven ascents available. The mean sounding is plotted in Fig. 13. The dew point values differ much more from sounding to sounding so that a composite has no meaning.

An air parcel from the surface layer with a temperature of 21 °C and a mixing ratio of 12 g/kg will, after saturation, and assuming adiabatic ascent, follow the moist adiabat $\theta_W = 18$ °C as indicated in Fig. 13. 21 °C was measured just south of Sardinia at 12.00 GMT (see Fig. 2c), and the mixing ratio of 12 g/kg corresponds to the mean value in the lowest 100 meters as observed from the Cagliari radiosonde ascent at 12.00 GMT 28 September. This ascent (not shown) takes place rather close to the center of the vortex, but over land, and the temperature at most levels corresponds to a value between the moist-adiabats $\theta_W = 17$ °C and $\theta_W = 18$ °C. We may assume, therefore, that the inner core has a vertical temperature distribution corresponding to $\theta_W \simeq 18$ °C or perhaps a little more. This in fact can be directly verified by the 1000/500 mb thickness map from 00.00 GMT 1 October (Fig. 12), where the warm core is clearly seen. Assuming a temperature distribution following a moist adiabat, the maximum thickness in the center of the warm core, ~5620 gpm, corresponds to a θ_W slightly above 18°C. From Fig. 13, we can conclude that the cloud top temperature of the most active cumulonimbus should be somewhat lower than −50°C. This indeed is verified by satellite measurements (Fig. 14): the region with intense convection is quite symmetric and the innermost part corresponds to a temperature of −52 to −54°C. Returning to the mean sounding (Fig.

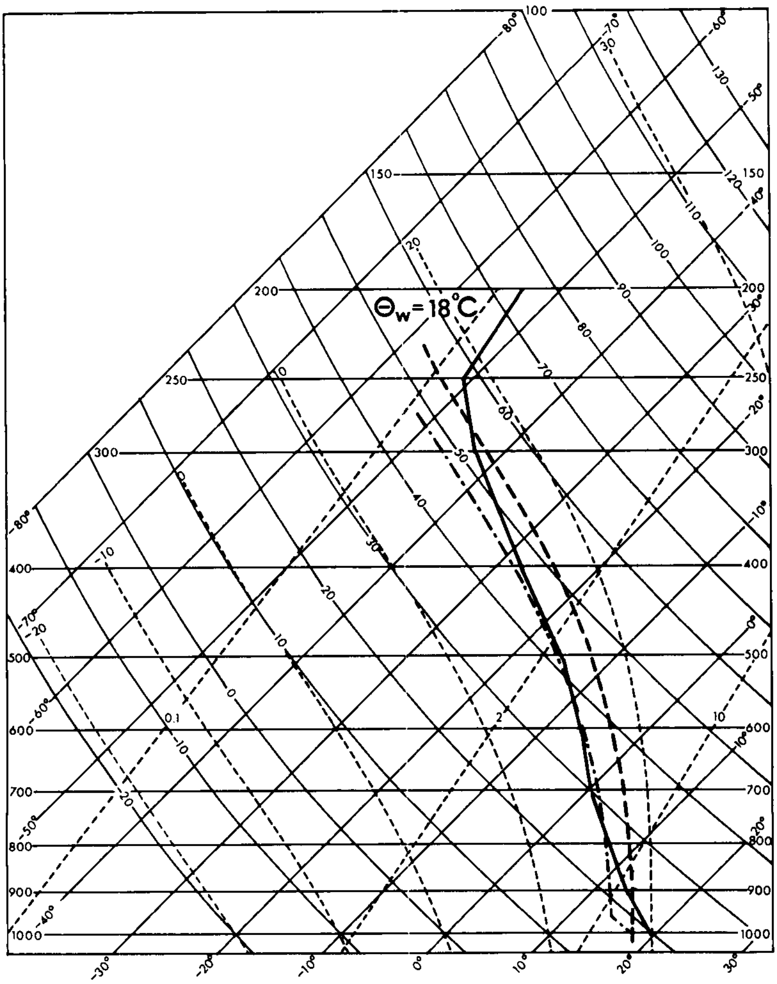

Fig. 13. Mean sounding (solid line), representative for conditions outside the core region of the subsynoptic vortex. The moist-adiabat $\theta_W = 18\,°C$ is shown by the dashed curve. The dash-dotted line shows the temperature of surface air ascending with a surface temperature 2.5 °C lower than that corresponding to the mean sounding. The ascent up to 960 mb is assumed to be dry-adiabatic and moist-adiabatic beyond that level.

13), we note that the stratification is conditionally neutral or stable from 700 mb upwards. In order for convection to proceed, the atmosphere below 700 mb must be conditionally unstable and sufficiently moist. The sea surface temperature and the moisture close to the surface are therefore important parameters for the development of the vortex and, all other things being equal, the system might not develop if the surface temperature is just a few degrees lower. The effect of a 2.5 °C decrease in the surface temperature for a particle starting its ascent at the surface has been illustrated in Fig. 13. The large positive area defined by the mean sounding and the $\theta_W = 18\,°C$ curve, corresponding to a substantial amount of CAPE, completely disappears if the surface temperature is decreased 2.5 °C (assuming the same cloud base in the two cases). This supports the notion in Subsection 4.1 that the vortex starts weakening at 18.00 GMT 29 September because it then enters a region where the sea surface is about 2.5 °C colder than further south (see Fig. 10).

The assumptions made above are tantamount

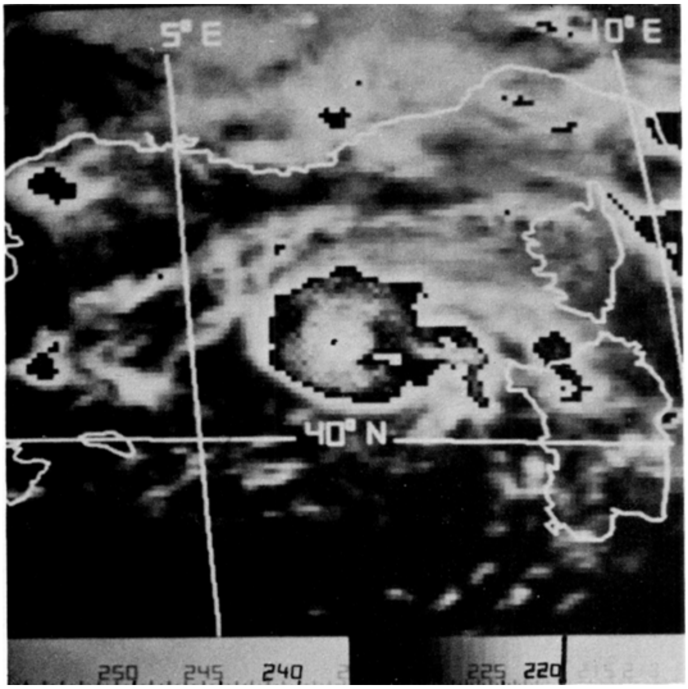

Fig. 14. METEOSAT infrared satellite image 12.00 GMT 29 September 1983, showing the cloud top temperatures of the mature vortex with enhancement of high level clouds as described in Fig. 3. The highest cloud tops (white) have equivalent black-body temperatures of -52 to -54°C.

to saying that our system during its vigorous phases consists of a central inner warm core with a temperature corresponding approximately to $\theta_w = 18$°C and a slightly colder environment corresponding to the mean sounding shown in Fig. 13. The temperature increment from the outer to the inner part of the vortex between 900 mb and 300 mb can easily be found from Fig. 13. Taking the increments for every 100 millibars and computing the mean, we find $\Delta\overline{T} \simeq 2.3$°C. The corresponding mean temperature of the moist adiabat $\theta_w = 18$°C is $\overline{T} \simeq 265$°K. Now, integrating the hydrostatic equation between 900 mb and 300 mb and differentiating with respect to $\overline{T}$ we find the following expression for the pressure decrement Δp_0 at the surface due to a mean temperature increment $\Delta\overline{T}$

$$\Delta p_0 = -gHp_0 \Delta\overline{T}/(R\overline{T}^2). \tag{1}$$

H is the height difference between the 300 and 900 mb surfaces, R the gas constant and g gravity. Inserting the quantities on the right-hand side, we find

$$\Delta p_0 = 4.4\,\Delta\overline{T}\ \text{mb}, \quad \text{i.e.,} \quad \Delta p_0 \simeq 10\ \text{mb}. \tag{2}$$

The exact value of the pressure perturbation is difficult to determine from observations, but 10 mb is realistic. At 06.00 GMT 28 September (Fig. 2b) for example, the central part of the low between Sardinia and the Tunisian coast must be considered as the "perturbation". As discussed in the foregoing the convection at this particular time seems to be very intense giving rise to the maximum pressure fall which we can expect due to hydrostatic warming. At this time the surface pressure at the center is close to 1000 mb which corresponds to a maximum pressure perturbation of about 10 millibars as predicted by the expression above. A similar good example can be found at 12.00 GMT 30 September when the center has made landfall on Corsica. Due to frictionally enhanced convection, the central pressure in the inner region has dropped to about 1005 mb. Apart from the region immediately around the vortex, the pressure gradient is very small over a very large area where the pressure is

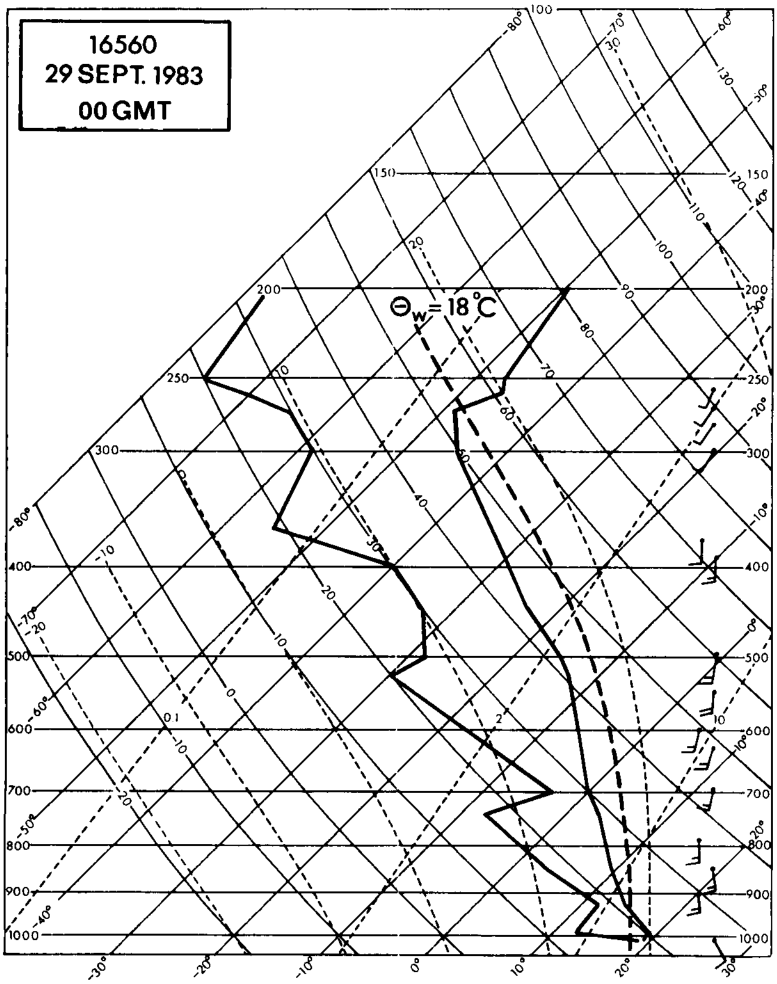

Fig. 15. Cagliari radio sounding 00.00 GMT 29 September 1983. The moist adiabat $\theta_W = 18°C$ is shown by the dashed curve. Winds are given in the conventional way.

about 1015 mb (see Fig. 2f), i.e. again we find a pressure perturbation of about 10 mb corresponding to the theoretically derived value.

4.3. *The dynamics of the vortex and the upper air wind data*

It has been implied in the foregoing that the axis of the vortex is approximately vertical like in a tropical cyclone and that the system has a warm core. Accordingly, the horizontal wind should blow from the same direction but with decreasing speed for increasing height. For large heights, it eventually may blow from the opposite direction corresponding to a reversal from cyclonic to anticyclonic flow. Since we have no data which tell us how temperature varies as a function of distance from the center of the vortex at different levels we cannot apply the thermal wind equation but only make a qualitative assessment.

The ascent from Cagliari of 00.00 GMT 29 September (Fig. 15), shows an almost unidirectional wind from the surface up to 250 mb and the wind speed is almost constant up to 400 mb, beyond which it decreases and becomes very weak at 300 mb and above. The ascent from Rome, 12.00 GMT 1 October (not shown), also shows a unidirectional or slowly turning and decreasing wind through a deep layer. Thus the horizontal wind varies with height in a way that qualitatively corresponds to a warm core structure of the vortex.

In the following, we will discuss the satellite-derived wind data and see how they fit together with the routine observations and the warm core model including the assumption of a vertical vortex axis.

On 28 September, the vorticity at low levels is strong near the center and weak at high levels (Figs. 6a, b). The fields, however, are still somewhat disorganized.

On 29 September, when the system is in its most steady phase far away from any coastline, we observe a well-organized structure. Both the low level cyclonic (positive) relative vorticity center and the main high level anticyclonic (negative) relative vorticity center coincide with the position of the surface pressure center. Also the highest clouds with minimum cloud top temperatures of -52 to -54°C are found in this region (Fig. 14). The upper level flow (Fig. 8b) is pronounced anticyclonic over the center of the vortex. The observations therefore support the point of view that the vortex has a warm core around a vertical axis.

On 30 September, landfall takes place around 09.00 GMT and the vortex tightens at low levels (Fig. 6e) corresponding to the increased inflow towards the center as a result of the increased surface friction. An even more remarkable consequence is seen at upper levels where the anticyclonic region now has been replaced by a cyclonic rotation with positive relative vorticity (Fig. 6f). Note that the center of the upper level cyclonic circulation is almost vertically above the low level vorticity and the surface center, i.e., the axis of the vortex is not sloping with height. Corresponding to the transformation from anticyclonic to cyclonic relative vorticity (Figs. 6d, f), high-level convergence is now observed around the vortex (Fig. 8c). The major mechanism responsible for this complete transformation is probably an increased vertical transport of the low level angular momentum due to the increased convection. Because of the weak trough which stretches from southern France in a south-easterly direction (Fig. 8d), the fields at this time are not quite as symmetrical as 24 hours before.

At 12.00 GMT 1 October, the low level vortex has regained some of its symmetry, and the intense high level cyclonic rotation has considerably diminished (not shown) reflecting that the vortex is partly recovering from the "shock" due to the passage across Corsica. The vortex is also clearly discernable at the surface map (not shown) and a ship reports surface winds of 15 m s^{-1} close to the center. There are important differences, however, between the situation of 1 October and two days before when the vortex was best developed. On 1 October, the vortex consists mainly of low level clouds with only a few scattered cumulonimbus complexes. With the conceptual model outlined above in mind all this indicates the beginning of decay of the system.

5. Summary and concluding remarks

The development of a subsynoptic vortex over the Mediterranean has been followed for several days. The major tool for the study were METEOSAT images from the visible and infrared spectrum, and wind data from low- and high-levels obtained by tracking cloud elements in these images. By means of the derived vorticity and divergence fields, and by routine observations, it has been possible to draw some qualitative conclusions about the dynamics of the system upon which a conceptual model can be based. Satellite images and surface observations document that the subsynoptic vortex forms in the central part of a synoptic scale low of modest intensity. Deep convection is observed in the region prior to the formation of the vortex which most probably is caused by a rapid spin-up due to intense convection of pre-existing vorticity associated with the synoptic scale low. A similar mode of formation of intense small-scale vortices embedded in lows of a somewhat larger dimension has been observed for polar lows (Økland, 1987).

Around noon on 29 September, a cirrus shield caps the vortex indicating intense and deep convection. The vortex at this time is characterized by a vertical axis and an upper level anticyclonic divergent flow corresponding to a warm core structure. Observations show that the vertical temperature distribution in the warm core (approximately) corresponds to that given by the $\theta_W = 18$°C moist adiabat. The hydrostatic effect of the formation of a warm core of that strength corresponds to a decrease of the surface pressure of the order of 10 mb, in accordance with what is actually observed.

Later on 29 September, the vortex starts to weaken. This happens when the vortex moves into a region with decreasing sea surface temperatures which may result in less CAPE being available for the disturbance. During the second landfall at Corsica at 30 September, the vortex temporarily intensifies. After the crossing of Corsica, however, the convection associated with the vortex becomes less widespread and more shallow than before, and the vortex weakens until it disappears after the final landfall at the Tunisian coast.

It is unlikely that baroclinic instability plays any role for the formation and continued existence of the vortex. Convection on the other hand is an important factor and the large amount of CAPE indicates that some kind of CISK may be the driving mechanism of this quasi-steady vortex (Emanuel, 1983).

6. Acknowledgements

This project has partly been financed by the German Research foundation DFG. Special thanks have to be given: to J. LeBer, ESA-ESOC, who provided the METEOSAT data; to Mr. Rattei and Dr. König operating the ISM at DFVLR; to Mrs. P. Dell'Anna, Free University of Berlin, and Mrs. A. Skjoldbo, The Danish Meteorological Institute, for finishing the drawings. We also wish to thank the French Meteorological Institute which supplied copies of their surface maps, and the Institut National de la Météorologie Tunisienne.

A METEOSAT film scene showing the complete history of the case has been prepared at ZEAM, Free University of Berlin, in cooperation with ESA and CDZ-Film Berlin. It is available through C. Zick.

REFERENCES

Billing, H., Haupt, I. and Tonn, W. 1983. Evolution of a hurricane-like cyclone in the Mediterranean Sea. *Beitr. Phys. Atmos. 56*, 508–510.

Emanuel, K. A. 1983. Elementary aspects of the interaction between cumulus convection and the large scale environment. In: *Mesoscale meteorology—theories, observations and models* (eds. D. K. Lilly and T. Gal-Chen). D. Reidel Publishing Company, 551–575.

Ernst, J. A. and Matson, M. 1983. A Mediterranean tropical storm? *Weather 38*, 332–337.

Hasler, A. F., Shenk, W. E. and Skillman, W. 1976. Wind estimates from cloud motions: phase 1 of an in situ aircraft verification experiment. *J. Appl. Meteorol. 15*, 10–15.

Mayengon, R. 1984. Warm core cyclones in the Mediterranean. *Mariners Weather Log 28*, 6–9.

METEOSAT Operations Advisory Group, 1979. METEOSAT cloud winds quality. Available from ESA-ESOC, Darmstadt, F.R. Germany.

Økland, H. 1987. Heating by organized convection as a source of polar low intensification. *Tellus 39A*, 398–408.

Rasmussen, E. 1985. A case study of a polar low development over the Barents Sea. *Tellus 37A*, 407–418.

Shenk, W. E. and Kreins, E. R. 1970. A comparison between observed winds and cloud motions derived from satellite infrared measurements. *J. Appl. Meteorol. 9*, 702–710.

Suomi, V. E. (principal investigator), 1975. *Man-computer interactive data access system (McIDAS)*. Final Rep. NASA contract No. NAS 5-2396, Space Sci. Eng. Center, Univ. of Wisconsin, 255 pp.

Zick, C. 1983. Method and results of an analysis of comma cloud developments by means of vorticity fields from upper tropospheric satellite wind data. *Meteorol. Rdsch. 36*, 69–84.